IEEE Access
Multidisciplinary | Rapid Review | Open Access Journal

Received February 20, 2021, accepted March 2, 2021, date of publication March 12, 2021, date of current version March 23, 2021.

Digital Object Identifier 10.1109/ACCESS.2021.3065685

Expert System-Based EMI Modeling Method for IGBT in Electric Drive System of EV

XIAOSHAN WU[1], XIAOHUI SHI[2], JIN JIA[2], YONG CHEN[3,4], (Senior Member, IEEE), AND XU LI[2]

[1]School of Automotive Engineering, Chongqing University, Chongqing 401331, China
[2]Vehicle Engineering Institute, Chongqing University of Technology, Chongqing 400054, China
[3]School of Automation Engineering, University of Electronic Science and Technology of China, Chengdu 611731, China
[4]Institute of Electric Vehicle Driving System and Safety Technology, University of Electronic Science and Technology of China (UESTC), Chengdu 611731, China

Corresponding authors: Xiaoshan Wu (wxs_bernice@163.com) and Yong Chen (ychencd@uestc.edu.cn)

This work was supported in part by the National Key Research and Development Program of China under Grant 2018YFB0106101, and in part by the Key Research and Development Program of Science and Technology Major Theme Project of Chongqing under Grant cstc2018jszx-cyctzxX0005.

ABSTRACT In the working process of the electric drive system, the transient, high-amplitude, high-frequency voltage and current generated by the turn-on and turn-off of the IGBT (Insulated Gate Bipolar Transistor) are the most important sources of electromagnetic interference in EVs (electric vehicles). To this end, this paper proposes an EMI (Electromagnetic interference) modeling method for IGBT power modules of electric drive systems, which can realize accurate simulation of EMI source characteristics. First, an expert system based on IGBT model library is proposed. Then the expert system is used to simulate the characteristic curves provided in the IGBT module datasheet and extract the key parameters. Based on the expert system, an IGBT behavioral model is established, and a double-pulse simulation circuit is built to evaluate the simulation waveforms of the collector-emitter voltage, gate-emitter voltage and collector current during the two pulse switching periods. At the same time, measure the collector-emitter voltage, gate-emitter voltage and collector current test waveforms collected in the above simulation test on the built double-pulse test circuit, and compare the turn-on and turn-off processes of the simulation and test respectively to evaluate the accuracy of the EMI source model. Finally, to further test the universality of the model, the IGBT behavior model and the double pulse simulation circuit are established on the Simulink platform, and the accuracy of the model is evaluated by comparing with the test waveform. The comparative analysis results show that the proposed EMI source modeling method for IGBT power module has good versatility and accuracy.

INDEX TERMS Electric drive system, IGBT power module, electromagnetic interference.

I. INTRODUCTION

As the power source of electric vehicles, the electric drive system is also the main source of high amplitude and high frequency EMI. The high-voltage inverter circuit is mainly an integrated IGBT power module, which is packaged by 6 IGBTs and 6 freewheeling diodes. High power, miniaturization and integration are the key features of IGBT power modules [1]. Due to the physical packaging structure, many parasitic parameters are inevitably introduced into them, affecting dynamic characteristics of the IGBT in the switching process, and even amplifying EMI Level. Therefore, it is significant to establish an accurate EMI source model of IGBT power module to further analyze the EMI of IGBT.

The associate editor coordinating the review of this manuscript and approving it for publication was Wenjie Feng.

Compared with physical models with complicated parameter acquisition and solving process [2], [3], behavioral models are more suitable for engineers to design and develop systems [4], [5]. Denz P [4] *et al.* proposed a simple parametric IGBT behavior model, which can roughly characterize the switching characteristics of IGBTs. Turzynski and kulesza [5] designed a behavioral model library of the MOSFET infrastructure, which changes the parameters based on the basic structure, to characterize more complex switching characteristics. In ref. [6] a SPICE-based IGBT behavior model modeling and simulation platform are constructed to provide design engineers with IGBT rapid evaluation tools.

Based on previous studies, the architecture of the IGBT behavior model is relatively clear. However, since the switching characteristic parameters of the IGBT are nonlinear, it is difficult to establish an accurate model by matching the switching characteristics with the limited parameters.

In addition, parasitic parameters of the IGBT power module will significantly affect the switching characteristics of the IGBT [7]–[9], which undoubtedly increases the difficulty of accurate modeling. For the IGBT model, the consistency between the double-pulse simulation and the test results is the ultimate mean to verify the modeling accuracy [10], [11].

Based on the IGBT datasheet provided by the module manufacturer, this study employs numerical fitting methods to extract the key parameters of the IGBT behavior model. And the IGBT behavior model is established based on the expert system, aiming at the upper and lower arms of the IGBT power module (single bridge arm), containing 1 IGBT and 1 freewheeling diode. Then an IGBT double-pulse test platform is built, and the accuracy of the EMI source model is evaluated through double-pulse simulation and test waveform comparison. In order to test the universality of the model, based on the datasheet parameters and the key parameters extracted, the IGBT behavior model is established on the Simulink platform, and the accuracy of the EMI source model is also evaluated by comparing the double pulse simulation with the test waveform. The flow is shown in Figure 1, in which blue boxes correspond to each heading.

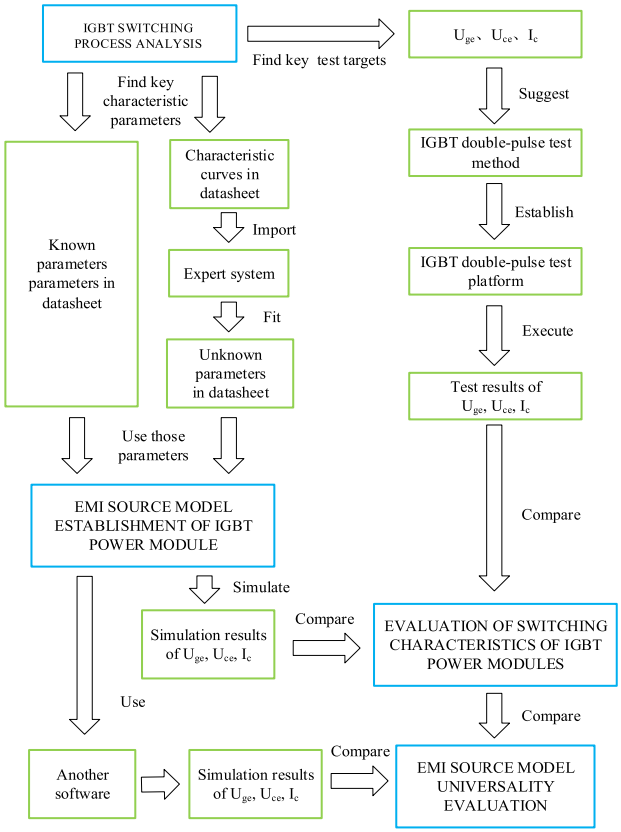

FIGURE 1. The flow of this article.

II. IGBT SWITCHING PROCESS ANALYSIS

A. ANALYSIS OF THE OPEN PROCESS

IGBT gate capacitance C_{ge} and C_{gc} play an important role in the IGBT turn-on process, which can be divided into 4 stages, as shown in Figure 2.

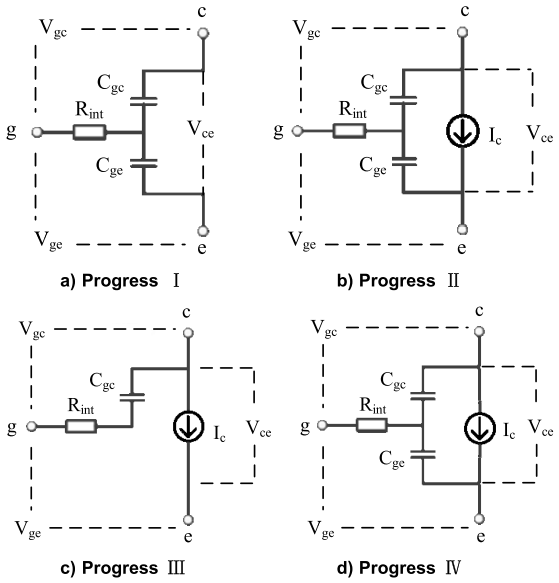

FIGURE 2. Turn-on progress analysis for IGBT (equivalent circuit).

1) Phase I: The external driving voltage charges the IGBT gate capacitances C_{ge} and C_{gc}, and the IGBT gate voltage V_{ge} gradually rises to the threshold voltage $V_{ge(th)}$. However, at this time, the IGBT is turned off.
2) Phase II: The IGBT gate voltage V_{ge} exceeds the threshold voltage $V_{ge(th)}$, the IGBT starts to turn on, and the collector current I_c increases; due to the presence of parasitic inductance, the collector-emitter voltage V_{ce} will decrease to a certain extent.
3) Stage III: Due to the Miller effect, the gate plateau voltage appears, and the driving voltage only charges the capacitor C_{gc}; V_{ce} continues to drop to close to the saturation voltage drop $V_{ce(sat)}$.
4) Stage IV: V_{ce} continues to drop to the saturation voltage drop $V_{ce(sat)}$ and remains unchanged, the IGBT is in a fully conductive state; the Miller effect disappears, the driving voltage charges the capacitors C_{ge} and C_{gc}, and the IGBT gate voltage continues to rise. Until the drive voltage.

In fact, the 4 stages of the IGBT turn-on process can be equivalent to the charging process of the external driving voltage V_g to the equivalent input capacitance C_{in} of each stage, the relationship can be formulated as:

$$L_g C_{in} \frac{d^2 v_{ge}(t)}{dt^2} + R_g C_{in} \frac{dv_{ge}(t)}{dt} + v_{ge}(t) = V_{gh} \tag{1}$$

where L_g means the gate loop inductance; R_g denotes the gate drive resistance, including internal gate resistance and external resistance; V_{gh} is the high level of the drive voltage V_g; $V_{ge(t)}$ means the IGBT gate voltage.

The equivalent input capacitance C_{in} is:

$$\begin{aligned} C_{in} &= \frac{dQ_g}{dv_{ge}} = \frac{C_{ge} dv_{ge} + C_{gc}\left(dv_{ge} - dv_{ce}\right)}{dv_{ge}} \\ &= C_{ge} + (1 - \frac{dv_{ce}}{dv_{ge}}) C_{gc} \end{aligned} \tag{2}$$

Additionally, the gradually increasing collector current I_c in phase II is controlled by the gate voltage and the transconductance g_f, as:

$$I_c(t) = g_f(v_{ge}(t) - V_{ge(th)}) \tag{3}$$

where g_f represents the transconductance of the IGBT.

B. ANALYSIS OF THE SHUTDOWN PROCESS

The turn-off process of the IGBT is opposite to the turn-on process, and is also divided into 4 stages, as shown in Figure 2. At this time, the gate voltage $V_{ge(t)}$ of each stage is similar to formula (1), except that the driving voltage high level V_{gh} needs to be changed to the driving voltage low level V_{gl}. What is more, when $V_{ge(t)}$ drops below the threshold voltage $V_{ge(th)}$, the collector current I_c of the IGBT will gradually drop to zero in the form of a tail current, which is approximately an exponential decay, as:

$$I_{tail}(t) = \alpha I_{c(on)} e^{-(t-t_0)/\tau} \tag{4}$$

In the formula, α is the current drop factor of the NPN transistor in the IGBT; $I_{c(on)}$ is the on-state current of the IGBT; t_0 is the time when the tail current starts; τ is the tail time constant.

III. EMI SOURCE MODEL ESTABLISHMENT OF IGBT POWER MODULE

A. IGBT BEHAVIOR MODEL STRUCTURE ANALYSIS

The high-voltage inverter circuit of the electric drive system adopts a three-phase full-bridge structure, which integrates 6 IGBT switches and 6 freewheeling diodes on one board, is regarded an IGBT power module. The model of the IGBT power module studied is Infineon FS820R08A6P2B [12].

IGBT is a complicated non-linear component and is difficult to model accuracy. Generally speaking, there are mainly numerical models, semi-numerical models, physical models, analytical models, and behavioral models. Among them, most of the parameters required for behavioral models can be extracted from datasheets, which are very suitable for engineering applications. Therefore, the IGBT behavior model is established via expert system, and the behavior model is shown in Figure 3.

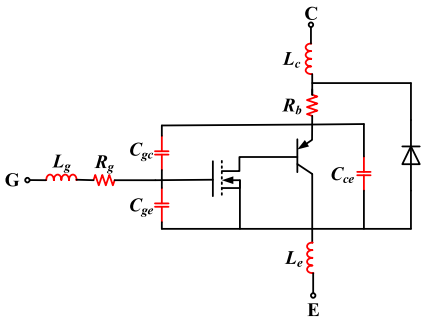

FIGURE 3. Equivalent circuit of IGBT behavior model.

B. IGBT BEHAVIOR MODEL PARAMETER EXTRACTION AND ESTABLISHMENT

According to the datasheet, $R_g = 0.7\Omega$, $R_b = 0.75$ mΩ, $L_g = 8$ nH, $L_c = L_e = 4$ nH, and other parameters are obtained by numerical fitting.

The IGBT static characteristics of consist of output characteristics, transfer characteristics, capacitance characteristics, gate charge characteristics and diode volt-ampere characteristics. Dynamic characteristics contain tail current characteristics, diode reverse recovery current characteristics, and dynamic characteristics exist in the actual switching waveform.

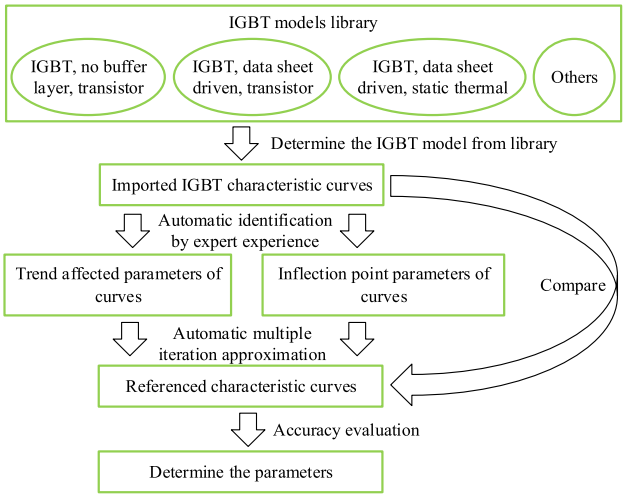

FIGURE 4. Main structure of this expert system.

Output characteristics describe the relationship between collector-emitter voltage (V_{ce}) and collector current (I_c); transfer characteristics describe the relationship between gate-emitter voltage (V_{ge}) and I_c; currently, research, standards and manufacturers at home and abroad. In the production process, the inter-electrode capacitance curve is not directly used, but the capacitance characteristic curve including the input capacitance C_{ies}, the output capacitance C_{oes} and the reverse transmission capacitance C_{res} is utilized to illustrate the relationship C_{ies}, C_{oes}, C_{res} and V_{ce} respectively, in which the inter-electrode capacitance The calculation formulas of C_{ge}, C_{gc}, C_{ce} and C_{ies}, C_{oes}, C_{res} are [13]:

$$\begin{cases} C_{ies} = C_{ge} + C_{gc} \\ C_{oes} = C_{gc} + C_{ce} \\ C_{res} = C_{gc} \end{cases} \tag{5}$$

In addition, the gate charge characteristics of the IGBT describe the relationship between the gate charge Q_g and V_{ge}; the tail current characteristics describe the relationship between the tail current I_t and the time t in the measured switching waveform; the diode volt-ampere characteristics describe the relationship between the diode voltage V_d and the current I_d; The diode reverse recovery current

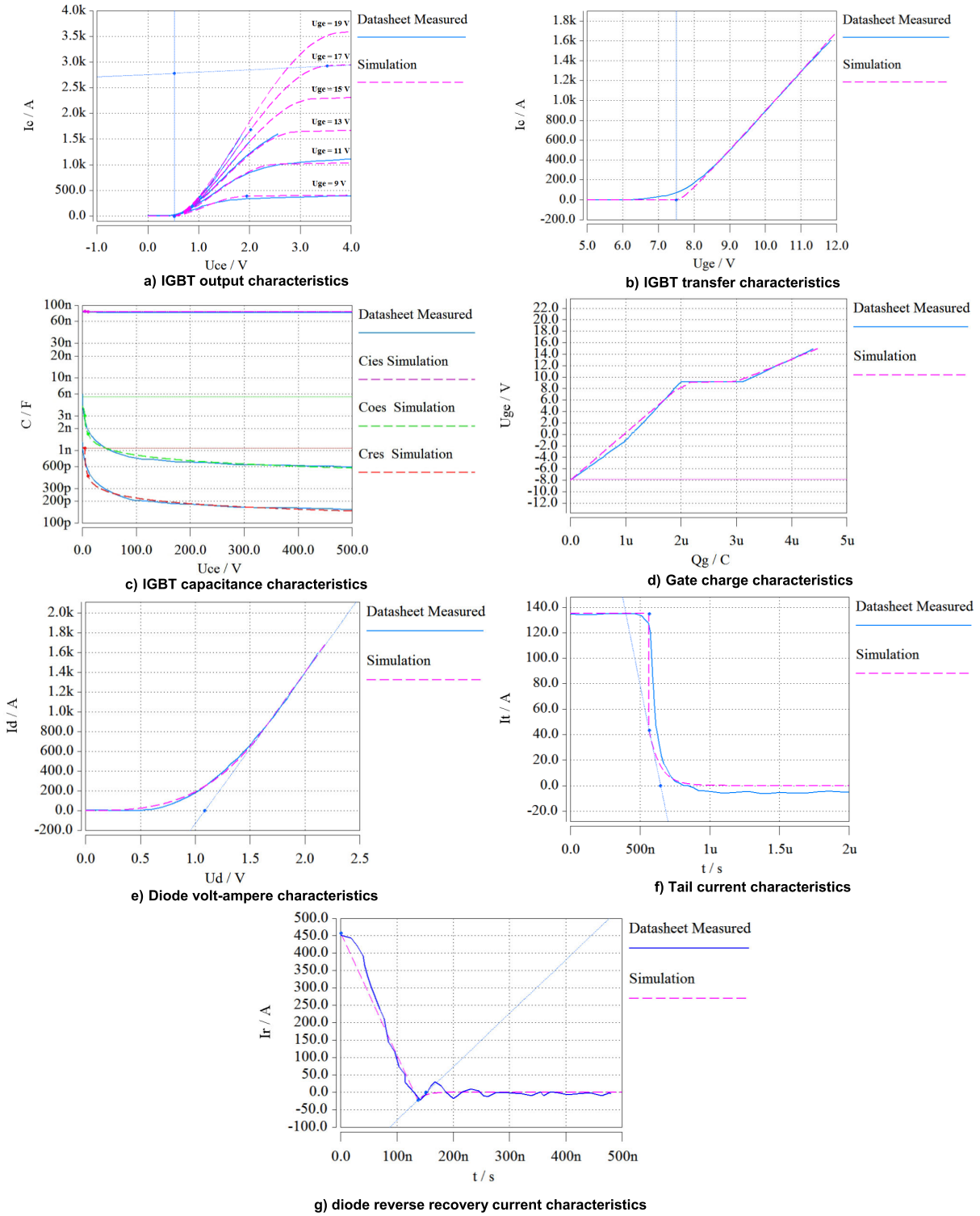

FIGURE 5. Fitting effect of IGBT switching characteristics.

characteristic describes the relationship between the diode reverse recovery current I_r and the time t in the measured switching waveform.

The so called expert system is a logical method system to achieve fast modeling, which can be regarded as a combination of "knowledge base" and "inference machine" [14]. An expert system for IGBT EMI characteristic modeling is proposed, of which the main structure is shown in Figure 4. The proportional integral (PI) program is used to fit the characteristic curves [15].

Through the scanning function of the expert system, the IGBT output characteristic test curves, transfer characteristic test curves, capacitance characteristic test curves, gate charge characteristic test curves, diode V-A characteristic test curves, diode reverse test curves provided in the datasheet at 25° C and 150° C, the tail current characteristic test curves and the recovery current characteristic test curves are imported into the IGBT model. Then the software (inference machine) fits the closest switching characteristic parameters to each curve through numerical iteration. The fitting effect ofIGBT curves switching characteristics are shown in Figure 5 (take the characteristics at 150° C as an example).

Analyze the fitting effect of the above characteristic curves:

1) The established IGBT behavior model can well reflect the static characteristics of the actual IGBT, has a consistent trend, and has a low error; since the capacitance characteristics and the gate charge characteristics are mutually affected, to ensure accurate capacitance characteristics, sacrifice Certain fitting accuracy of gate charge characteristics.
2) The dynamic characteristic curve is extracted according to the actual switching waveform. The tail current characteristic and the diode reverse recovery characteristic coexist with this waveform, and the overall trend is basically consistent.

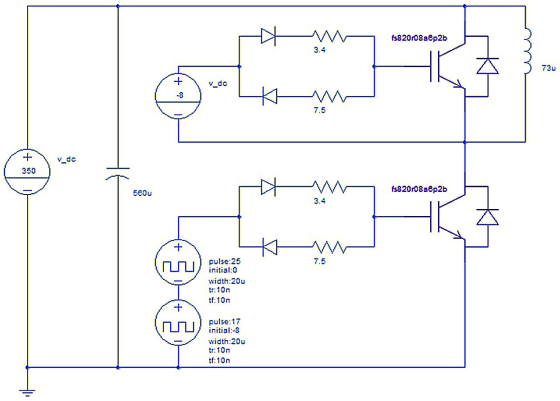

FIGURE 6. Double-pulse simulation circuit.

IV. EVALUATION OF SWITCHING CHARACTERISTICS OF IGBT POWER MODULES

A. IGBT DOUBLE PULSE SIMULATION CIRCUIT ESTABLISHMENT

The double pulse simulation circuit established in expert system is shown in Figure 6. The system voltage (also named $\boldsymbol{V_{dc}}$) is set to $\boldsymbol{U_{dc}} = 340$V, the on-pulse time is set to $\boldsymbol{t_{on}} = 20\mu$s, and the pulse amplitude is + 17 V/ − 8 V. The above-mentioned IGBT behavior models are imported into the double pulse simulation circuit, and the gate voltage (also named $\boldsymbol{V_{ge}}$) $\boldsymbol{U_{ge}}$, collector-emitter voltage (also named $\boldsymbol{V_{ce}}$) $\boldsymbol{U_{ce}}$ and collector current $\boldsymbol{I_c}$ of the lower-arm IGBT are measured, and the results are shown in Figure 7.

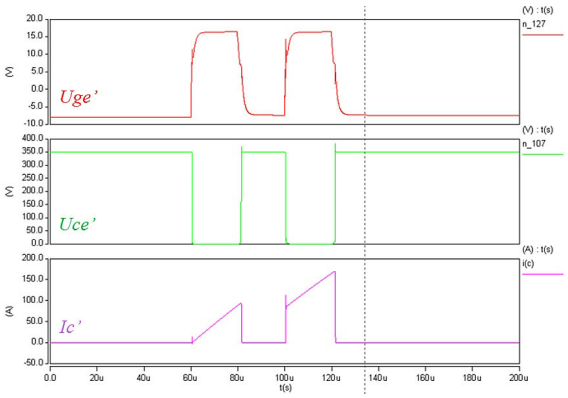

FIGURE 7. Double-pulse simulation results.

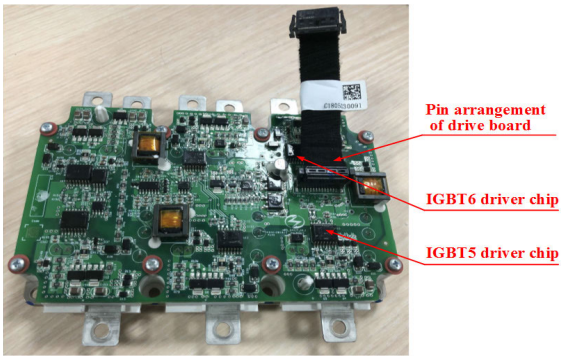

FIGURE 8. IGBT drive module and drive board assembly (sample).

B. IGBT DOUBLE PULSE TEST CIRCUIT CONSTRUCTION

Figure 8 shows the IGBT drive module and drive board loaded in the motor controller of the actual electric drive system. The test circuit uses a bridge arm of the sample (including two IGBTs and two diodes) to build an IGBT double pulse peripheral circuit for double pulse testing to evaluate and verify the switching characteristics of IGBTs.

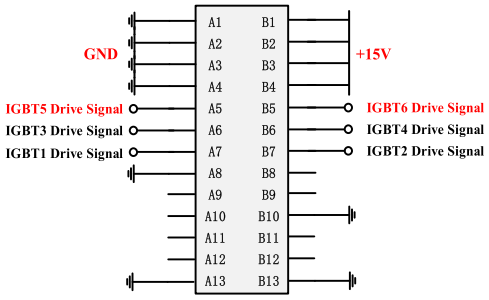

FIGURE 9. Driver board input pins.

The pin definition of the driver board sample is shown in Figure 9 where IGBT5 and IGBT6 are the upper and lower bridges of the same bridge arm. Supply $\boldsymbol{U_{dc}} = +15$ V direct current to the drive board, and $\boldsymbol{U_{ge}}$ of all IGBTs is − 8 V at this time. Use a signal generator to send a + 5 V/0 V double pulse signal to the IGBT6 drive signal interface. Through the isolation and amplification function of the drive chip and drive circuit, + 15 V / − 8 V can be generated on the gate of IGBT6 (actually approximately + 17 V/− 8 V) drive

signal. At the same time, the signal generator needs to send a 0 V DC signal to the IGBT5 drive signal interface to release the upper and lower bridge arm interlocking procedures. The double pulse test sample and the peripheral circuit are shown in Figure 10.

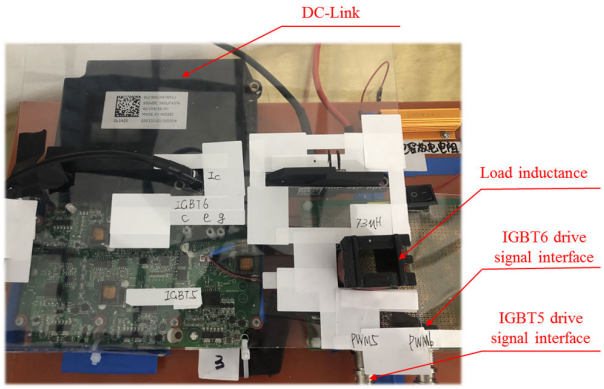

FIGURE 10. Double-pulse test layout.

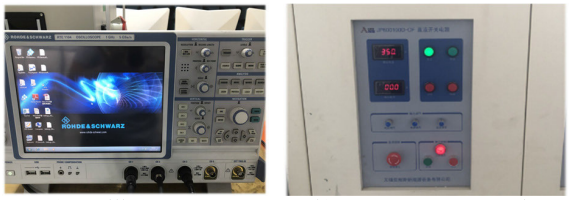

a) Oscilloscope b) HV DC power supply

FIGURE 11. Main equipments for double-pulse test.

The Main equipments required in the experiment includes: an oscilloscope, a high-power DC power supply, two signal generators, a high-voltage differential probe, a high-current probe, and a common voltage probe (mainly shown in Figure 11). The model of oscilloscope is R&S RTE 1104 with four channels, 1 GHz bandwidth and 5 Gsa/s sampling rate; the model of large-current flexible probe is Cybertek 9300s model with nominal range It is 3000 A, the bandwidth is 30 MHz; the model of high-voltage differential probe is a Tektronix P5200A model with a nominal range of 1000 V and a bandwidth of 50 MHz.

In addition, the peripheral circuits in this article include a load inductance of 73 μH, a DC support capacitor of 560 μF, a drive resistance $\boldsymbol{R_{gon}} = 3.4\Omega$, $\boldsymbol{R_{goff}} = 7.5\Omega$, and a DC bus connection between the support capacitor and the IGBT power module consistent with the actual electric drive system. To ensure safety, the two ends of the supporting capacitor are connected to a power resistor through a switch, and the energy stored in the capacitor is consumed through the resistor after each test.

The system voltage is set to $\boldsymbol{U_{dc}} = 340$V, and the on-pulse time is set to $\boldsymbol{t_{on}} = 20\mu$s. The test site is shown in Figure 12. Use the double pulse test platform to test the IGBT switching characteristics are evaluated by a double pulse test platform, the test waveforms of $\boldsymbol{U_{ge}}$, $\boldsymbol{U_{ce}}$ and $\boldsymbol{I_c}$ are shown in Figure 13.

The actual test conditions are shown in Table 1. The power supply voltages of 340 V and 470 V are the rated

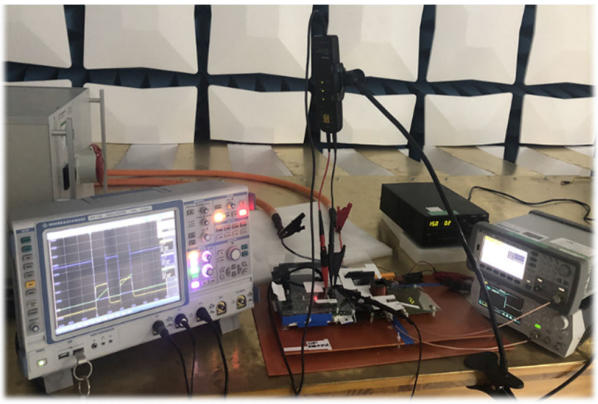

FIGURE 12. IGBT double-pulse test platform.

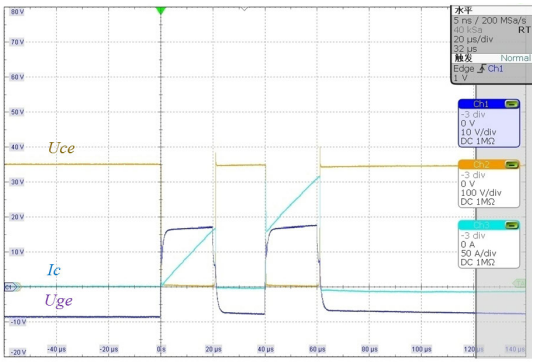

FIGURE 13. Double-pulse test result.

TABLE 1. Actual test conditions.

Working condition	Supply voltage	Single pulse time	Peak current (need to reach)
1	340 V	20 µs	150 A
2	340 V	35 µs	250 A
3	470 V	20 µs	200 A
4	470 V	65 µs	450 A

and peak working voltage of the actual electric drive system, respectively.

The simulation and test comparisons of IGBT switching characteristics under various operating conditions are shown in Figure 14-17.

It can be seen that under 4 different working conditions, the switching process simulation waveforms of the built IGBT behavior model are basically consistent with the test waveforms, and the IGBT model compares the voltage and current spikes (overshoot) during the actual IGBT turn-on and turn-off process. It is well presented and can correctly reflect the EMI characteristics of the bridge arm of the IGBT module, and the model has a preferable accuracy.

It should be mentioned that when testing $\boldsymbol{U_{ge}}$, the solder joints between the IGBT gate and the driver board are lengthened by the welding process to make the voltage probe hook the test point. This method introduces additional parasitic inductance, which makes $\boldsymbol{U_{ge}}$. During the switching process, the test waveform of the oscilloscope appeared in actual

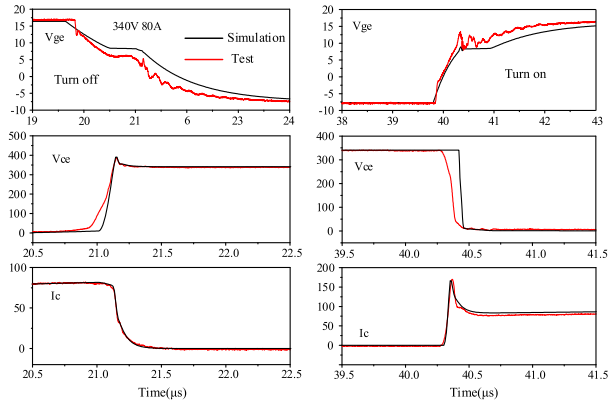

FIGURE 14. Simulation and experimental comparison of IGBT switching process under operating condition 1.

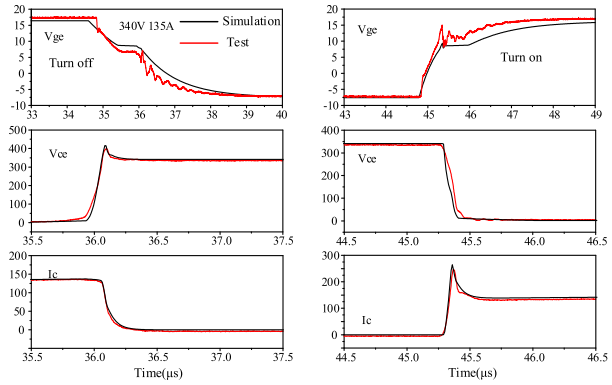

FIGURE 15. Simulation and experimental comparison of IGBT switching process under operating condition 2.

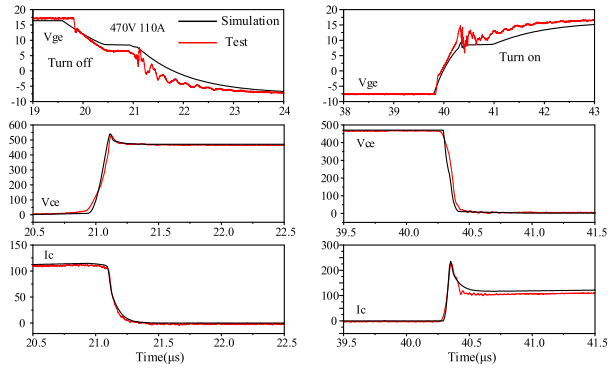

FIGURE 16. Simulation and experimental comparison of IGBT switching process under operating condition 3.

non-existent oscillation, but it did not affect the trend of U_{ge}. And U_{ge} test results under several working conditions are consistent.

In addition, there are still some differences between the results of simulation and testing in general. The errors also originate from the tiny parasitic resistances and parasitic inductances of power lines and contact points in the experimental platform. The simulation circuit does not consider these external parasitic parameters, therefore, these parameters can be regarded as random parameters introduced by the test platform.

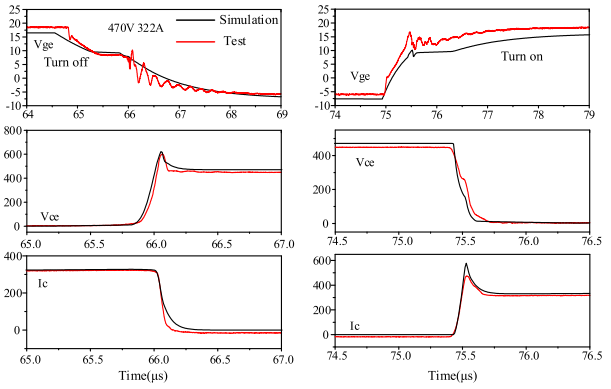

FIGURE 17. Simulation and experimental comparison of IGBT switching process under operating condition 4.

temp	25	150
vt	7.52568	7.4816
von	0.606769	0.516604
a	0.00769579	0.001
b	0.00322125	0.00333964
x	5.73861	2.4617
y	1.2222	1.58485
z	1.10097	0.610836
vaf	21.0569	59.404
rg	0.664104	0.7
tauon	1n	1n
tauoff	63n	80n
beta	4.11236	0.475229
rb	0.00685092	0.001
taurb	1.91752u	5u
dccg	213.861p	304.227f
rdon	586.828u	653.859u
rdoff	318598.0	318599.0

vd	1.22054	1.08395
n	3.99583	3.00992
rrk	7862.45	13964.7
rrtau	59.0006n	87.9997n
>> Capacitances		
cres0	130.403n	
cres1	4.60933n	
cres2	398.68p	
coes0	135.092n	
coes1	9.25552n	
coes2	1.55735n	
cies0	251.133n	
v1	2.26451	
v2	18.3172	
m	0.317271	
vge0	7.76	

FIGURE 18. IGBT behavior model parameters in expert system.

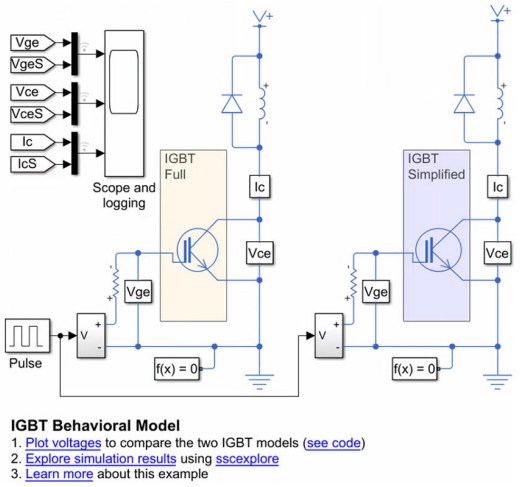

FIGURE 19. IGBT behavior model in Simulink library.

V. EMI SOURCE MODEL UNIVERSALITY EVALUATION

Compared with the expert system, the Simulink software platform has been widely used for simulation. Generally, system-level EMI simulation of electric drive systems is more convenient in Simulink. In order to evaluate the universality of the established IGBT behavior model, the parameters obtained by expert system numerical fitting in the behavior model (as shown in Figure 18) and the parameters provided in the IGBT datasheet are correspondingly imported into the Simulink behavior model as shown in Figure 19.

The description of parameters in Figure 18 are shown in Table 2.

TABLE 2. Description of parameters in expert system model.

z	Output characteristic quasilinear region constant
V_{af}	Output characteristic saturation slope constant
r_g	Gate internal resistance
t_{auon}	Base area/drift area time constant at turn-on
t_{auoff}	The base area/drift area time constant at turn-off
beta	Current amplification of bipolar transistor
r_b	Base area/drift area resistance at turn-off
t_{aurb}	Base/drift resistance time constant
d_{ccg}	Miller capacitance correction term
r_{don}	Diode on-resistance
r_{doff}	Diode off-resistance
V_d	Diode knee voltage
n	Coefficient effecting diode on-resistance and off-resistance
r_{rk}	Reverse recovery amplitude constant
r_{rtau}	Reverse recovery time constant
C_{res0}, C_{oes0}, C_{ies0}	The maximum value on each capacitance curve
C_{res1}, C_{oes1}	The reverse capacitance and the output capacitance when the collector-emitter voltage is equal to V_1
C_{res2}, C_{oes2}	The reverse capacitance and the output capacitance when the collector-emitter voltage is equal to V_2
V_1	V_{ce} value greater than zero corresponding to the point (C_{res1}, V_1) on the reverse capacitance curve
V_2	V_{ce} value greater than zero corresponding to the point (C_{res2}, V_2) on the reverse capacitance curve
m	Parameter affecting the profile of capacitance curves
V_{ge0}	Voltage defining the nonlinear C_{ge} capacitance in the negative gate charge region

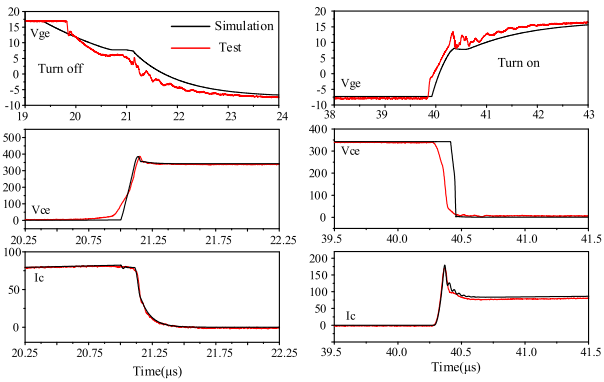

FIGURE 20. Simulation and experimental comparison of IGBT switching process under operating condition 1.

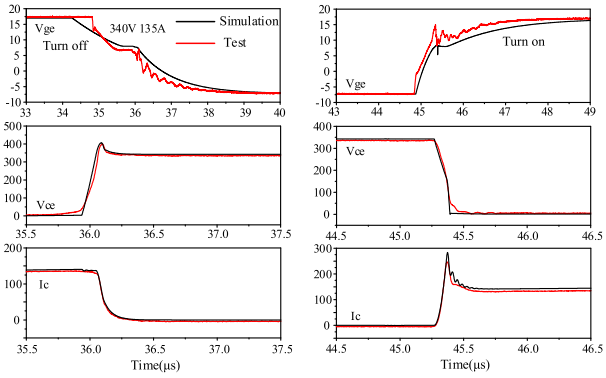

FIGURE 21. Simulation and experimental comparison of IGBT switching process under operating condition 2.

As mentioned in the previous section, the dual-pulse simulation circuit is also established in Simulink software.

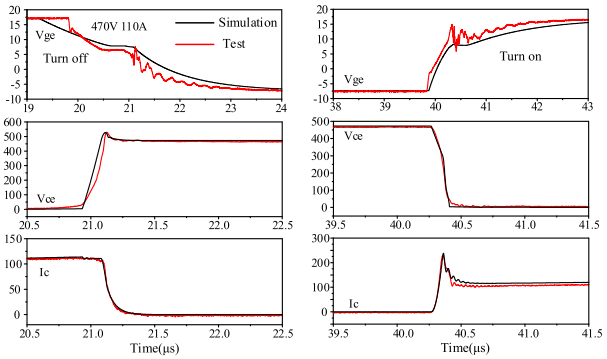

FIGURE 22. Simulation and experimental comparison of IGBT switching process under operating condition 3.

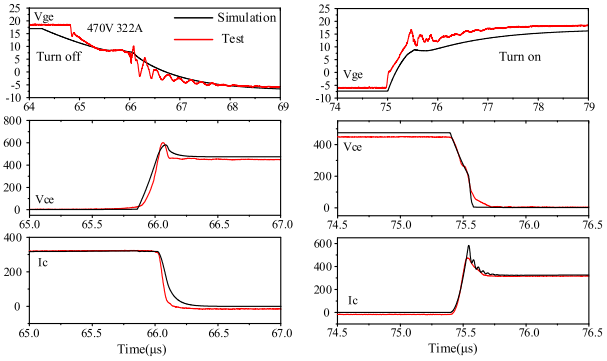

FIGURE 23. Simulation and experimental comparison of IGBT switching process under operating condition 4.

The simulation and test comparison of IGBT switching characteristics under various operating conditions are shown in Figure 20 - 23.

It can be observed from Figure 14-17 and Figure 20-23 that the IGBT behavior model based on the Simulink simulation platform and the IGBT behavior model based on the expert system have basically the same switching characteristics, and both can accurately determine the EMI characteristics of the IGBT module bridge arm. The model has strong versatility.

VI. CONCLUSION

In this paper, aiming at the EMI source of the IGBT power module of the electric drive system of electric vehicles, a set of modeling simulation and experimental verification methods with certain versatility and accuracy are proposed.

The main research work includes the following contents:

1) Based on limited modeling parameters and input conditions, the IGBT modeling expert system is used to fit the key parameters of the IGBT behavior model which are not included in the datasheet. And the IGBT behavior model is established on the expert system.

2) The accuracy of the model is evaluated by the IGBT double pulse test. It has been verified that the voltage and current spikes (overshoot) in the actual IGBT turn-on and turn-off process can be better presented, and the interference source characteristics are more consistent.

3) A behavior model is established by Simulink based on the parameters obtained by expert system and the parameters provided by the IGBT datasheet. The IGBT behavior models established by the two simulation platforms have basically the same switching characteristics, and both can accurately determine the EMI characteristics of the IGBT module bridge arms.

The simulation and test results demonstrate that the EMI source model establishment and test verification methods of the IGBT power module proposed in this paper have strong versatility and engineering guiding significance for the further system-level or vehicle-level EMI modeling.

REFERENCES

[1] G. Liu, K. Li, Y. Wang, H. Luo, and H. Luo, "Recent advances and trend of HEV/EV-oriented power semiconductors—An overview," *IET Power Electron.*, vol. 13, no. 3, pp. 394–404, 2020, doi: 10.1049/iet-pel.2019.0401.
[2] M. Cotorogea, "Physics-based SPICE-model for IGBTs with transparent emitter," *IEEE Trans. Power Electron.*, vol. 24, no. 12, pp. 2821–2832, Dec. 2009, doi: 10.1109/TPEL.2009.2030328.
[3] F. Chimento, N. Mora, M. Bellini, I. Stevanovic, and S. Tomarchio, "A simplified spice based IGBT model for power electronics modules evaluation," in *Proc. 37th Annu. Conf. IEEE Ind. Electron. Soc.*, Melbourne, VIC, Australia, Nov. 2011, pp. 1155–1160, doi: 10.1109/IECON.2011.6119471.
[4] P. Denz, T. Schmitt, and M. Andres, "Behavioral modeling of power semiconductors in modelica," in *Proc. 10th Int. Modelica Conf.*, Lund, Sweden, pp. 343–352, doi: 10.3384/ecp14096343.
[5] M. Turzynski and W. J. Kulesza, "A simplified behavioral MOSFET model based on parameters extraction for circuit simulations," *IEEE Trans. Power Electron.*, vol. 31, no. 4, pp. 3096–3105, Apr. 2016, doi: 10.1109/TPEL.2015.2445375.
[6] G. Sfakianakis, M. Nawaz, and F. Chimento, "A temperature dependent simple spice based modeling platform for power IGBT modules," in *Proc. IEEE Energy Convers. Congr. Expo. (ECCE)*, Pittsburgh, PA, USA, May 2014, pp. 2873–2879, doi: 10.1109/ECCE.2014.6953788.
[7] Y. Yang, Y. Wen, and Y. Gao, "A novel active gate driver for improving switching performance of high-power SiC MOSFET modules," *IEEE Trans. Power Electron.*, vol. 34, no. 8, pp. 7775–7787, Aug. 2019, doi: 10.1109/TPEL.2018.2878779.
[8] Y. Xu, C. N. M. Ho, A. Ghosh, and D. Muthumuni, "An electrical transient model of IGBT-diode switching cell for power semiconductor loss estimation in electromagnetic transient simulation," *IEEE Trans. Power Electron.*, vol. 35, no. 3, pp. 2979–2989, Mar. 2020, doi: 10.1109/TPEL.2019.2929113.
[9] J. Wang, H. S.-H. Chung, and R. T.-H. Li, "Characterization and experimental assessment of the effects of parasitic elements on the MOSFET switching performance," *IEEE Trans. Power Electron.*, vol. 28, no. 1, pp. 573–590, Jan. 2013, doi: 10.1109/TPEL.2012.2195332.
[10] Y. Tang and H. Ma, "Dynamic electrothermal model of paralleled IGBT modules with unbalanced stray parameters," *IEEE Trans. Power Electron.*, vol. 32, no. 2, pp. 1385–1399, Feb. 2017, doi: 10.1109/TPEL.2016.2542198.
[11] L. Zhang, X. Yuan, X. Wu, C. Shi, J. Zhang, and Y. Zhang, "Performance evaluation of high-power SiC MOSFET modules in comparison to Si IGBT modules," *IEEE Trans. Power Electron.*, vol. 34, no. 2, pp. 1181–1196, Feb. 2019, doi: 10.1109/TPEL.2018.2834345.
[12] *HybridPACK Drive Module FS820R08A6P2B Final Datasheet*, Infineon Technologies AG, Neubiberg, Germany, 2017.
[13] K. Tanya Gachovska, L. Jerry Hudgins, E. Santi, and A. Bryant, *Modeling Bipolar Power Semiconductor Devices*. Seattle, WA, USA: Morgan & Claypool, 2013, doi: 10.2200/S00483ED1V01Y201302PEL005.
[14] M. Agarwal and S. Goel, "Expert system and it's requirement engineering process," in *Proc. Int. Conf. Recent Adv. Innov. Eng. (ICRAIE)*, Jaipur, Rajasthan, May 2014, pp. 1–4, doi: 10.1109/ICRAIE.2014.6909306.
[15] S. E. Saravi, A. Tahani, F. Zare, and R. A. Kordkheili, "The effect of different winding techniques on the stray capacitances of high frequency transformers used in flyback converters," in *Proc. IEEE 2nd Int. Power Energy Conf.*, Johor Bahru, Malaysia, Dec. 2008, pp. 1475–1478, doi: 10.1109/PECON.2008.4762710.

XIAOSHAN WU was born in Sichuan, China, in 1987. She is currently pursuing the Ph.D. degree with the College of Vehicle Engineering, Chongqing University. Her main research interest includes vehicle electromagnetic compatibility technology.

XIAOHUI SHI was born in Chongqing, China, in 1963. He received the Ph.D. degree from the College of Vehicle Engineering, Chongqing University, Chongqing, China, in1994. He is currently the Director of the Automotive Intelligent Technology Research Institute of Chongqing Qingyan Institute of Technology. His main research interests include test methods, online detection techniques, virtual tests, and new sensors for major automotive components.

JIN JIA was born in Sichuan, China, in 1985. He received the German Doctor of Engineering degree from Dortmund Technical University, Germany, in June 2015. He studied under the supervision of Prof. Stephan Frei, an Internationally Renowned Expert in automotive electronics. From August 2015 to August 2018, he was the Deputy Director of the EMC Technology Center, China Automotive Engineering Research Institute Company Ltd. His main research interest includes vehicle electromagnetic compatibility technology. In June 2015, he was awarded the Excellent Grade from the Doctoral Defense of Engineering, Germany, and awarded the title of EMV2012 Young Engineer, Dusseldorf, Germany.

YONG CHEN (Senior Member, IEEE) was born in Sichuan, China, in 1977. He received the Ph.D. degree from Chongqing University, Chongqing, China, in 2007. He was a Visiting Scholar with The University of Adelaide, in 2013. Since 2015, he has been a Professor and the Ph.D. Supervisor with the School of Automation Engineering, and the Director of the Institute of Electric Vehicle Driving System and Safety Technology, University of Electronic Science and Technology of China (UESTC). He has published over 100 technical papers in journals and conferences, and 20 Chinese patents. His current research interests include power electronics and motor control.

XU LI was born in Sichuan, China, in 1978. He received the Ph.D. degree in electrical engineering from Chongqing University, Chongqing, China, in 2008. From July 2008 to March 2019, he worked with the Chang'an Automobile Group, Automotive Engineering Institute of China, as an Engineer, a Senior Engineer, and a Professorate Senior Engineer. From July 2009 to May 2013, he held a postdoctorate position with the Institute of Electrical Engineering, Chinese Academy of Sciences. From November 2015 to December 2016, he worked as a Visiting Scholar with the Electromagnetic Compatibility Laboratory, Missouri University of Science and Technology, Missouri, USA. He is currently a Professorate Senior Engineering with the School of Vehicle Engineering, Chongqing University of Technology, Chongqing. His main research interest includes vehicle electromagnetic compatibility technology.